Kinetic and Thermodynamic Studies of the Isothermal Curing Reaction of the Diglycidyl Ether of Bisphenol A/ Ni(II) Chelate System

M. Ghaemy, A. Omrani, A. A. Rostami

Department of Chemistry, Faculty of Science, Mazandaran University, Babolsar, Iran

Received 30 June 2004; accepted 21 November 2004
DOI 10.1002/app.22059
Published online in Wiley InterScience (www.interscience.wiley.com).

ABSTRACT: The curing reaction of a system consisting of a diglycidyl ether of bisphenol A (DGEBA) based epoxy and a new inorganic complex curing agent based on Ni(II) chelate with ethylendiamine (en) as a ligand was studied with an isothermal Fourier transform infrared (FTIR) technique. The hardener was prepared and characterized by means of FTIR spectroscopy, elemental analysis, and ICP–plasma techniques. The results of kinetic studies with two kinetic models, Horie et al. and Kamal, showed that the Kamal method gave the best fit to the experimental data. The overall values of the rate constants and activation energy for the DGEBA/$Ni(en)_3Br_2$ system were calculated. The activation energy of the curing process was also determined by an isoconversional method, which showed that with the progress of curing time, the activation energy increased. Further, the results obtained from thermodynamic studies give the entropy change of activation, which was more negative for the *n*th-order path, whereas the activation heat of the reaction was more negative for the autocatalytic path.
 J Appl Polym Sci 98: 1540–1547, 2005

Key words: curing of polymers; FTIR; kinetics (polym.); resins

INTRODUCTION

Epoxy resin is one of the most important polymeric materials as polymer matrices for composites and electronic components because of its excellent adhesive and dielectric properties. However, the curing reactions of epoxy resins are normally complex because many reactive processes occur simultaneously, and there are other parameters that increase the complexity of the curing reaction, such as vitrification and gelation phenomena and the change from chemical kinetic control to diffuse control in the progress of the curing reaction. Several methods have been used to improve the final properties of thermosetting materials. Recently, articles using the transition metal complexes as controllable curing agents for epoxy resins have been published.[1–3] Metal chelate–epoxy polymers have also offered several advantages, including superior thermal stability.[4] The kinetics of the curing of epoxy resin has been widely studied with isothermal and dynamic differential scanning calorimetry (DSC) and Fourier transform infrared (FTIR) techniques. Experimental data have been analyzed by homogeneous reaction models, normally with autocatalytic or *n*th-order mechanisms.[5–9] FTIR is one of the techniques that has been used[10–12] because it permits one to detect the variation of functional groups if the spectra are checked at consecutive periods of time. This is based on the fact that if the degree of conversion increases, the intensity of the absorption band of terminal groups decreases. However, kinetic study of thermoset resins is useful for a variety of applications, including shelf-life prediction and the optimization of processing conditions. These kinetic data also provide information for the curing cycles of epoxy resins to ensure that the adequately cured epoxy is able to meet the requirements of its end use.

The objects of this study were (1) to check the applicability of kinetic analysis with FTIR spectra for this new epoxy system; (2) to perform a kinetic study from which parameters such as reaction orders, rate constants, and active energies were determined; and (3) to perform a thermodynamic study with transition state (TS) theory where the amounts of enthalpy ($\Delta H^{\#}$), entropy ($\Delta S^{\#}$), and Gibbs free energy ($\Delta G^{\#}$) changes were also determined.

EXPERIMENTAL

Materials

Ethylendiamine (en) was obtained from Fluka and was purified before use. Nickel carbonate and chloride were also obtained from Fluka. The commercial epoxy resin, Epon 828, based on diglycidyl ether of bisphenol

Correspondence to: M. Ghaemy (ghaemy@umz.ac.ir).

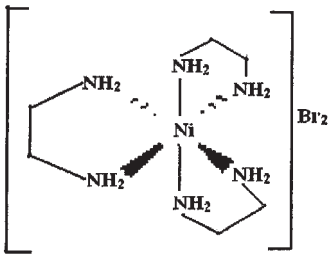

Figure 1 Structure of the $Ni(en)_3Br_2$ curing agent.

A (DGEBA), was supplied by Shell Chemical Co. and had an epoxy equivalent weight of 185 as determined by wet analysis.[10] A complete description of the complex curing agent preparation and characterization is given in our previous work.[13] Figure 1 shows the structure of the complex hardener used in this study. The elemental analysis of the curing agent and a comparison with the requested values are listed in Table I.

Sample preparation and characterization

The complex curing agent had to be dried completely *in vacuo* and ground to powder before mixing with the epoxy. The epoxy resin and curing agent (10 phr) were carefully mixed and stirred to provide a homogeneous mixture. From this homogeneous mixture, samples were prepared by the casting of a thin film on a potassium chloride plate, which was covered with another plate. The sandwich-like salt plate was placed in an oven with an exact temperature controller. FTIR spectra were monitored with the progress of the curing reaction with a Nicolet 550 Magna IR system at a 2-cm^{-1} resolution. The isothermal temperatures 150, 160, 170, and 180°C were used. The commercially recorded wave number range was from 600 to 4000 cm^{-1}. All of the solvents used in this work were degassed with high-purity nitrogen before use. For the $DGEBA/Ni(en)_3Br_2$ system, OMNIC software was used to process and calculate all of the data from the FTIR spectra.

RESULTS AND DISCUSSION

Kinetic studies

The curing of a thermoset and, particularly, epoxy resins involves the formation of a rigid three-dimensional network by a reaction between the oxirane ring

TABLE I
Elemental Analysis Data for $Ni(en)_3Br_2$

Complex	%C	%H	%Ni
Br_2	16.4 (16.57)	6.8 (6.44)	13.67 (13.5)

Requested values are shown in parentheses.

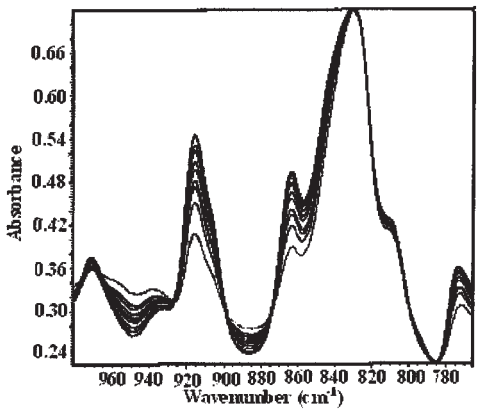

Figure 2 FTIR spectra of the $DGEBA/Ni(en)_3Br_2$ system at 150°C for different curing periods: 0, 9, 25, 35, 45, 65, 75, 85, and 95 min.

of the epoxy oligomer with hardeners that have more than two reactive functional groups. The chemistry of curing is initiated through the formation and linear growth of the chain, which soon begins to branch and then to crosslink. As the cure proceeds, the molecular weight increases rapidly. On the other hand, with the progress of the curing reaction, the concentration of epoxide groups (the absorption bands of the oxiran ring) decrease with a simultaneous increase in the concentration of hydroxyl groups. This breakdown of oxirane rings, which follows the progress of curing, can be performed by several mechanisms, including an autocatalytic one at low temperatures or at the initial times of the curing reaction (before the dissociation of the hardener), a reaction of active hydrogen atoms in the ligand at relatively high temperatures, and other reaction paths. FTIR spectroscopy is a powerful tool for monitoring and a more precise indicator of the extent of cure than DSC, as it directly measures the chemistry taking place rather than the heat evolved. Figure 2 shows a typical IR spectra of the $DGEBA/Ni(en)_3Br_2$ system for the isothermal temperature of 150°C, which was recorded for different periods of curing reaction. Various peaks of DGEBA were assigned;[14] of these peaks, the most important absorption was the epoxide group at 914 cm^{-1}. It was obvious that the primary amine peak at 1624 cm^{-1} and the epoxide group peak at 914 cm^{-1} decreased in size with increasing reaction time. By calculating the area under the latest peaks, we determined the conversion of these functional groups at different times. It was relatively easy to calculate the conversion of the epoxide group (α) because the peak was well separated from the other peaks. However, for primary amines, the absorbance peak at 3454 cm^{-1} could not be used for quantitative analysis because of severe overlapping with secondary amines (3367 cm^{-1}) and the expanded peak of hydroxyl groups produced during curing. In addition, there was unequal reactivity of the

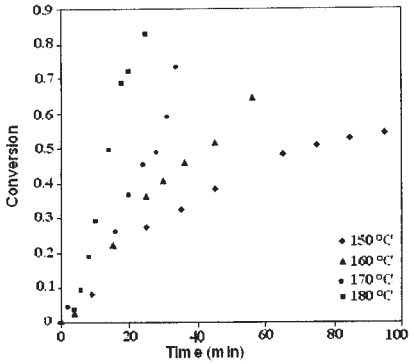

Figure 3 α in the DGEBA/Ni(en)$_3$Br$_2$ system at different isothermal temperatures.

primary and secondary amines in the bulk system; the primary amines had a higher reactivity than the secondary amines.

Generally, as shown in the previous figures, the intensity of the vibration band of the terminal epoxide groups decreased during the curing reaction and that was selected for quantitative analysis in this study. The band at 1245 cm^{-1} could be assigned to the aliphatic–aromatic ether linkage, and the bands at 1510 and 830 cm^{-1} could be assigned to *p*-phenylene groups. These last bands were not appropriate for kinetic analysis because of the overlapping of the spectra of the same isothermal temperature during different periods of time. The phenylene absorption peak at 830 cm^{-1} was used as a reference peak for the normalization of the epoxy absorption peak. From the spectra, we used a method derived from Beer's law[14,15] that was based on the ratio of the height of the characteristic peak (914 cm^{-1}) to reference the absorbance peak (830 cm^{-1}).

The degree of conversion at different isothermal temperatures was calculated and is plotted against time in Figure 3. The initial slope of the curves were steeper for higher temperatures, but next to that, the slope got smaller after a certain amount of time, particularly for lower temperatures, which could have been due to a diffusion-controlled reaction. As shown in Figure 3, α reached 40% after 1 h at 150°C, whereas it was almost 80% in less than 30 min at 180°C. The incomplete α was due to the vitrification of the epoxy resin. The increase in curing time was followed by an increase in the molecular weight, and because of this, the chains started branching and crosslinking, which hindered mobility, and consequently, crosslinking stopped. At all temperatures, the degree of conversion showed autoacceleration in the initial stages, as indicated by the slight positive curvature. Sewell et al.,[16] Nunez et al.,[17] and Barton[18] showed autoacceleration for similar epoxy systems. Figure 4 shows the reaction rate versus time at different isothermal temperatures. As shown, the reaction rate increased with temperature but dropped faster with increasing temperature. This may have been because at high conversions, the reaction was controlled by a diffusion mechanism. Also, as shown in Figure 4, the maximum rate of the reaction appeared at nonzero times, indicating that the cure reaction could not be described as an *n*th-order reaction mechanism.

One of the kinetic models that we have used to check the best fit to experimental data was proposed by Horie et al.[19] and is expressed as

$$d\alpha/dt = (k_1 + k_2\alpha)(1 - \alpha)^n \quad (1)$$

where α is the conversion of the epoxide group and k_1 and k_2 are the specific rate constants related to the noncatalytic and catalytic rate constants, respectively. The other kinetic model was proposed by Kamal,[20,21] who developed to the following semi-empirical equation:

$$d\alpha/dt = (k_1 + k_2\alpha^m)(1 - \alpha)^n \quad (2)$$

The reaction orders m and n are adjustable parameters, and the sum $m + n = 2$ has been adopted in most literature reports.[22,23] The introduction of the variable exponents m and n usually makes it possible to obtain a good fit to experimental data. The reduced rate (α°) is defined as

$$\alpha^\circ = (d\alpha/dt)/(1 - \alpha)^n = k_1 + k_2\alpha^m \quad (3)$$

The method is based on the search for values of m and n for the best linear fitting between the experimental and theoretical data. For the Horie model, the value of m in eq. (3) is equal to 1. The values of $d\alpha/dt$ and α were obtained from the experimental FTIR spectra of the studied system. Different values of n (0.5, 1, 1.5, and 2) were tried in eq. (3) to obtain the best linear fit to the experimental data. Plots of α° versus α for

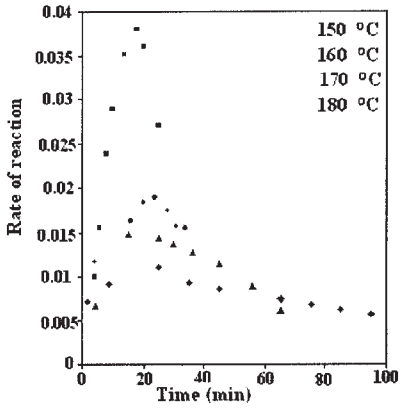

Figure 4 Plots of reaction rate against time for the different isothermal temperatures.

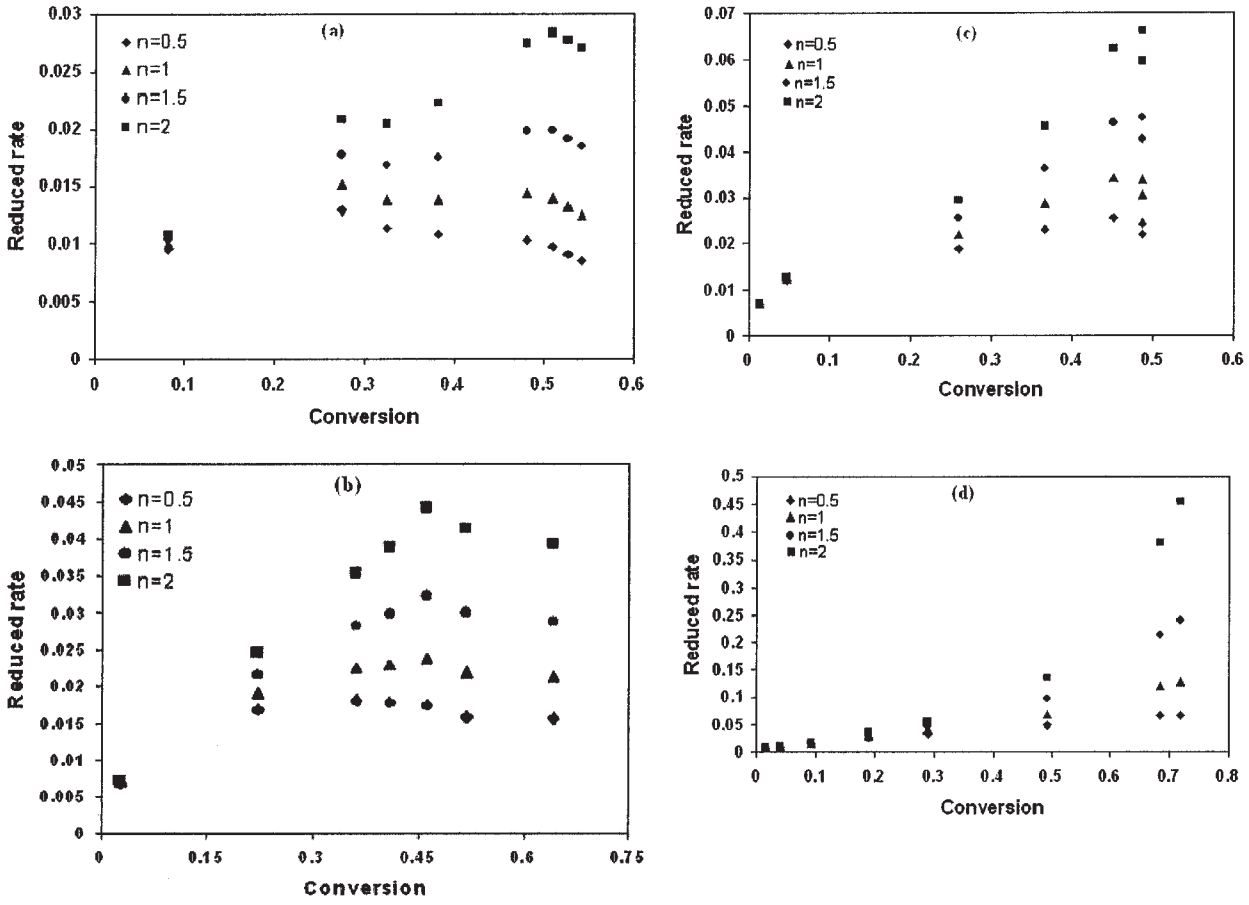

Figure 5 Plots of α° versus conversion for different n values(0.5, 1, 1.5, and 2) at various temperatures: (a) 150, (b) 160, (c) 170, and (d) 180°C.

different n values at four isothermal temperatures are shown in Figure 5(a–d). The results indicated that the best linear fitting was achieved when $n = 2$. For the Horie model, once this value was found, we concluded that the overall reaction order was 3. k_1 and k_2, obtained from the intercept and slope of the straight lines, resulted from a linear fitting of Figure 5. The values of the rate constants are listed in Table II.

There are several methods for the estimation of the four parameters (k_1, k_2, m, and n) in the Kamal equation.[24–26] These methods are based on assumptions that are limited to reactions where the total reaction order is known. The best calculative approach is the graphical–analytical method applied by Kenny.[25,27] We also used a similar method in this study. The isothermal curves (Fig. 4) in this study always gave a finite value of the reaction rate when extrapolated to zero time. This result was consistent with findings by other workers,[9,11,12] with a nonzero initial value for the autocatalytic reaction path, which attributed to certain reactions that were dominant only in the early stages of the curing reaction. The initial reaction rate in this study could be related to the fast catalytic polymerization of the epoxy oligomer by the complex curing agent.

TABLE II
Values of the Rate Constants Calculated with the Horie Model

Temperature (°C)	k_1 (min^{-1}), nth order	k_2 (min^{-1}), autocatalyzed
15	0.0034	0.0493
160	0.0051	0.0839
17	0.0067	0.1162
180	0.0093	0.1442

Therefore, at the start of the cure reaction ($t = 0$, where t is time, and $\alpha = 0$), eq. (3) simplifies to

$$[d\alpha/dt]_{t=0} = k_1 \tag{4}$$

One can directly determine the values of k_1 from the isothermal reaction curves, as plotted in Figure 4, by extrapolating to zero time. The observed k_1 values, given in Table III, ranged from 0.0028 to 0.0073 in the temperature range 150–180°C.

The integration and rearrangement of eq. (3) yields

TABLE III
Average Values of k_2, m, and n for the Isothermal Curing of the DGEBA/Ni(en)$_3$Br$_2$ System with the Kamal Model

Temperature (°C)	k_1 (min^{-1})	k_2 (min^{-1})	m	n	$m + n$
150	0.0028	0.039	0.69	1.94	2.63
160	0.004	0.062	0.89	1.5	2.39
170	0.0065	0.08	1.02	1.35	2.37
180	0.0073	0.18	1.16	1.2	2.36

$$\ln\{[(d\alpha/dt)/(1-\alpha)^n] - k_1\} = \ln k_2 + m \ln \alpha \quad (5)$$

The left side of this equation can be estimated if one considers a numerical value for n. Several different values of n over the range of $n = 0.1$–4, with a rate of 0.1, were tried in eq. (6). On the basis of the initial values of n and k_1, a plot of the left part of eq. (6) against ln α showed linear behavior with a possibility of the calculation of k_2 and m, respectively, as the intercept and slope of the straight line. This interactive procedure was repeated for different values of n to calculate the related values of k_2 and m with a computer program to find the best linear fit to experimental results. The final average values of n, m, and k_2 were determined and are listed in Table III. For the system under investigation, the values of m appeared to increase somewhat with increasing isothermal temperature.

To check the models for the best fit to the experimental data, plots of the reaction rate versus time (at different isothermal temperatures) were made, as shown in Figure 6(a,b).

The results show that both the Kamal and Horie models gave the best fit to the experimental results. We were not able to use isothermal temperatures higher than 180°C because of limitations in the thermal stability of the epoxy resin before curing. The activation energies (E_a's) corresponding to the two kinetic paths (nth order and autocatalytic) and the frequency factor (A), were obtained from the Arrhenius plots of ln k against $1000/T$ (where T is the absolute temperature) and are shown in Figure 7. The obtained values are listed in Table IV.

The small deviation from the linear behavior at high conversion (Fig. 7) may have been related to the diffusion control of the curing reaction at higher temperatures and longer times. However, it is possible to improve the results if one considers a diffusion factor in the experimental data, which was beyond the scope of this study.

To estimate the dependence of E_a on conversion for the experimental results of the studied epoxy system, we used the isoconversional method. However, without knowing the exact reaction mechanism, it was reasonable to assume that the reaction rate at a given time was only a function of the conversion. That means

$$d\alpha/dt = k f(\alpha) \quad (6)$$

where k is the rate constant and is usually assumed to be of the Arrhenius form as follows:

$$k = k_0 \exp(-E_a/RT) \quad (7)$$

where k_0 is a constant and $f(\alpha)$ is the conversion dependence function. The time to reach a specific con-

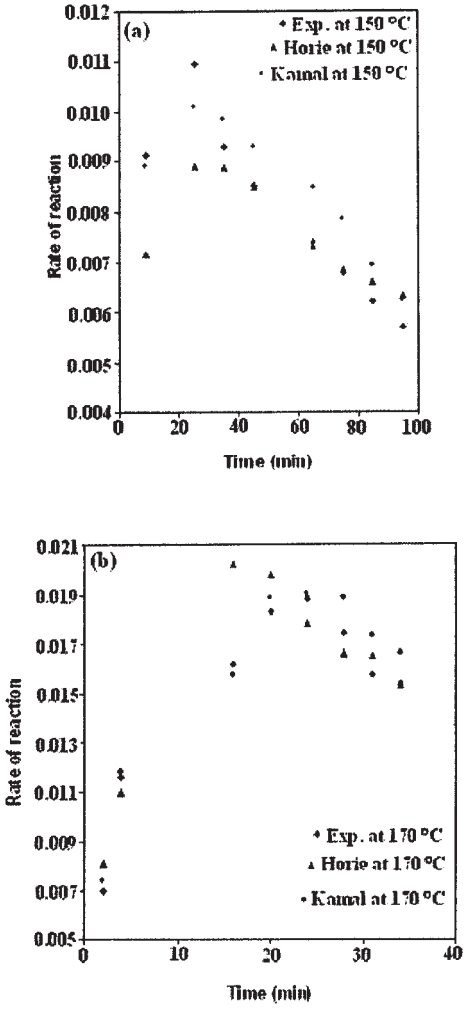

Figure 6 Typical plots of reaction rate versus time. Comparison of experimental data with the Horie and Kamal models at (a) 150 and (b) 170°C.

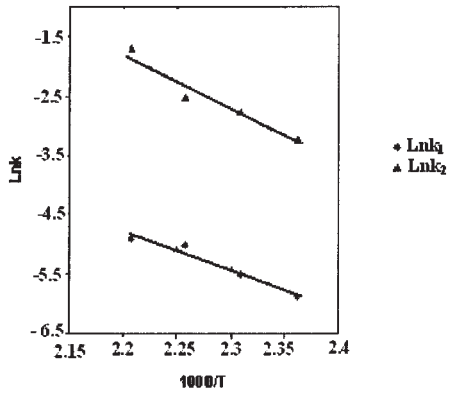

Figure 7 Arrhenius plots of ln k against $1000/T$.

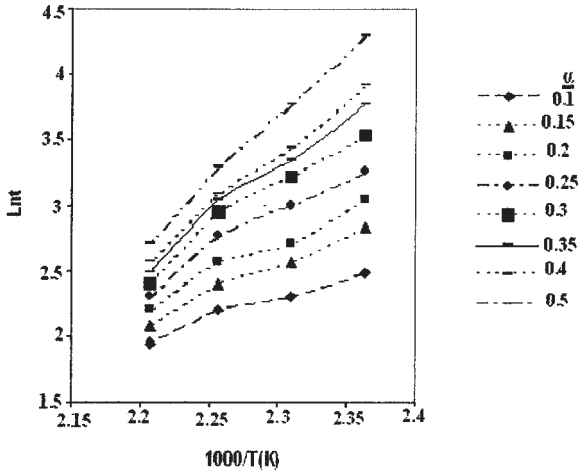

Figure 8 Plots of ln t versus the reciprocal of temperature at various conversions.

version at a constant temperature is determined by integrated form of eq. (6), which often appears as

$$g(\alpha) = \int_0^{\alpha} d\alpha/f(\alpha) = \int_0^{?} Kdt = Kt \qquad (8)$$

where $g(\alpha)$ is the integrated form of the conversion dependence function.

Replacing eq. (7) with eq. (8), we have

$$t = t_0 \exp(-E_a/RT) \qquad (9)$$

where t_0 is constant for a fixed conversion. This means that the time to reach the same conversion fraction at different isothermal temperatures has an Arrhenius temperature dependence. This was used to analyze the isothermal FTIR experiments. With eq. (9), the E_a's were obtained from the slope of the linear portion of ln t versus $1000/T$. Plots at eight constant values of α (i.e., 0.1, 0.15, 0.2, 0.25, 0.3, 0.35, 0.4, and 0.5) are shown in Figure 8. Also, the E_a dependence to conversion is shown in Figure 9. From the results obtained here, it appears that the E_a's were sensitive to the time of cure process and varied over the range of 27.4 kJ/mol for the initial time of curing to 83.04 kJ/mol at 50% conversion.

TABLE IV
Values of E_a and A Calculated from the Slope of the Linear Plots in Figure 7 with the Rate Constants in Table III

	E_a (kJ/mol)	ln A
nth order	53.79	9.4359
Autocatalytic	77.04	18.597

Thermodynamic study

One of the most important theories used to determine the changes of $\Delta S^{\#}$, $\Delta H^{\#}$, and $\Delta G^{\#}$ for thermosets is the TS or activated complex (AC) theory.[28] On the basis of this theory, a TS or an AC ($ABC^{\#}$) that is in equilibrium with the reactants (A, B, and C) must be formed before the formation of the final product (P). For two or three molecular systems, this theory can be shown with the following equations:

$$A + B + C \overset{K^{\#}}{\rightleftharpoons} ABC^{\#} \overset{k}{\rightarrow} P \qquad (10)$$

$$A + B \overset{K^{\#}}{\rightleftharpoons} AB^{\#} \overset{k}{\rightarrow} P \qquad (11)$$

The equilibrium constant ($K^{\#}$) for the activation of the TS can be written as

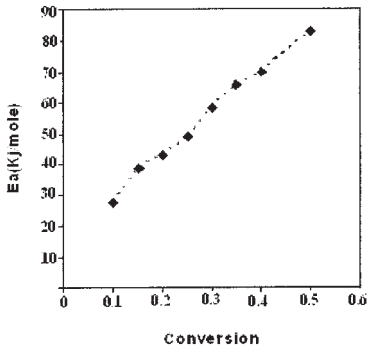

Figure 9 E_a versus conversion for the DGEBA/Ni(en)$_3$Br$_2$ system.

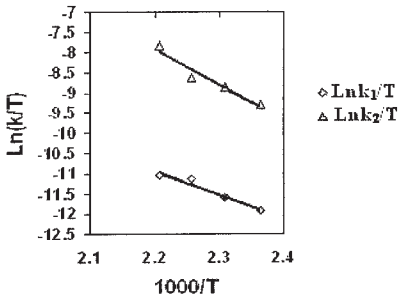

Figure 10 Arrhenius plots of $\ln(k/T)$ against $1000/T$.

$$K^{\#} = [ABC]^{\#}/[A][B][C] \text{ or } K^{\#} = [AB]^{\#}/[A][B] \quad (12)$$

where [A], [B], [C], and $[ABC]^{\#}$ represent the concentration of A, B, C, and the AC, respectively. On the other hand, absolute reaction rate theory has shown that

$$k[A][B][C] = [ABC]^{\#}K_BT/h \quad (13)$$

where k is the specific reaction rate constant for the formation of product; K_B and h are Boltzmann and Planck's constants, respectively; and T is the absolute temperature. Because the concentration of the AC ($ABC^{\#}$) is not measurable, it can be replaced with the last two equations:

$$k[A][B][C] = K^{\#}[A][B][C]K_BT/h$$

The specific reaction rate constant can be shown as follows:

$$k = K^{\#}\, K_BT/h \quad (14)$$

This equation is fundamental in the calculation of the thermodynamic parameters in the curing reaction of epoxy systems based on TS theory. $K^{\#}$ is related to the $\Delta G^{\#}$ as follows:

$$\Delta G^{\#} = -RT \ln K^{\#} = \Delta H^{\#} - T(\Delta S^{\#}) \quad (15)$$

where $\Delta H^{\#}$ is the activation heat of reaction, $\Delta S^{\#}$ is the entropy change of activation, and R is the gas constant. $\Delta G^{\#}$ can also be written as

$$\Delta G^{\#} = -RT \ln (kh/K_BT) = \Delta H^{\#} - T(\Delta S^{\#}) \quad (16)$$

Solving eq. (16) for k

$$k = K_BT/h \exp(-\Delta G^{\#}/RT) \quad (17)$$

Or

$$k = K_BT/h \exp(\Delta S^{\#}/R)\, exp(-\Delta H^{\#}/RT) \quad (18)$$

TABLE V
$\Delta H^{\#}$ and $\Delta S^{\#}$ Values

	$\Delta H^{\#}$ (kJ/mol)	$\Delta S^{\#}$ (J mol^{-1} k^{-1})
nth order	−50.158	−177.93
Autocatalytic	−73.41	−101.77

Taking natural logarithms of the last equation, one can obtain

$$\ln (k/T) = \ln[K_B/h \exp(\Delta S^{\#}/R)] - \Delta H^{\#}/RT \quad (19)$$

The plot of $\ln(k/T)$ versus $1/T$ gives a linear line with a slope of $\Delta H^{\#}/R$ and an intercept on the y axis equal to $\ln[K_B/h \exp(\Delta S^{\#}/R)]$. These thermodynamic quantities were calculated with rate constants obtained from the Kamal method (Table III). The corresponding plots are shown in Figure 10, and the values of $\Delta H^{\#}$ and $\Delta S^{\#}$ are given in Table V.

As shown, $\Delta S^{\#}$ was more negative for the nth-order path, whereas $\Delta H^{\#}$ is more negative for the autocatalytic one. With the equation $\Delta G^{\#} = \Delta H^{\#} - T\Delta S^{\#}$, the values of nth-order path and autocatalytic ($\Delta G_{n\text{-path}}$ and ΔG_{auto}) at various curing temperatures were calculated and are listed in Table VI. The values of $\Delta G^{\#}$ in Table VI show that for the DGEBA/$Ni(en)_3Br_2$ system, the autocatalytic mechanism is more favorable.

CONCLUSIONS

The kinetic parameters (degree of conversion, reaction rates, and E_a's) of the curing reaction of DGEBA/$Ni(en)_3Br_2$ system were obtained with the isothermal FTIR method. FTIR spectroscopy is a powerful tool for monitoring the kinetic reaction of an epoxy/hardener system. The intensity of the oxiran band at 914 cm^{-1}of the spectra is suitable for quantitative analysis. At all temperatures, the degree of conversion increased when the intensity of the band at 915 cm^{-1}decreased.

The reaction order and rate constants were determined with the Horie model. The best linear fit to the

TABLE VI
$\Delta G^{\#}$ Values for Two Reaction Mechanism Paths

Temperature (K)	$\Delta G^{\#}_{n\text{th path}}$ (kJ/mol)	$\Delta G^{\text{auto}}_{\#}$ (kJ/mol)
378.15	17.126	−34.41
388.15	18.906	−33.91
398.15	20.7	−32.89
408.15	22.46	−31.87
418.15	24.24	−30.85
428.15	26.02	−29.83
438.15	27.8	−28.8
448.15	29.6	−27.78
458.15	31.4	−26.78

experimental results was achieved for $n = 2$, and it was concluded that the overall reaction order was 3.

The Kamal kinetic model was also used to fit $d\alpha/dt$ versus α plots. The values of kinetic parameters were determined with this model for different isothermal experiments. The overall reaction order ($m + n$) was between 2 and 3, close to 2.5. The best fitting model, plots of the reaction rate versus time, at different isothermal temperatures was checked for the experimental data. We concluded that Kamal model is the one that best fit the experimental results of the studied isothermal curing temperatures.

The E_a's corresponding to the two kinetic mechanisms (nth order and autocatalytic) were obtained, 53.7 and 77 kJ/mol, respectively, from the Arrhenius plots of ln k versus $1000/T$ with rate constants obtained from Kamal model. On the basis of the dependence of E_a on the conversion, the calculated E_a showed a strong dependence on the extent of the curing reaction.

Finally, we concluded from thermodynamic studies that the autocatalytic path was dominant for the formation of the AC.

References

1. Brown, J.; Hamerton, I.; Howlin, B. J. J Appl Polym Sci 2000, 75, 201.
2. Hamerton, I.; Hay, N. J.; Howlin, J. B.; Jepson, P.; Mortimer, S. J Appl Polym Sci 2001, 80, 1489.
3. Hamerton, I.; Hay, N. J.; Herman, H.; Howlin, J. B.; Jepson, P. J Appl Polym Sci 2001, 84, 2411.
4. Kurnoskin, A. V. J Appl Polym Sci 1992, 46, 1509.
5. Osihi, T.; Fujimoto, M. J Polym Sci Part A: Polym Chem 1992, 30, 1821.
6. Turi, E. A. Thermal Characterization of Polymer Materials; McMillan: New York, 1987.
7. Prime, R. B. Polym Eng Sci 1973, 13, 365.
8. Wang, C. S.; Lin, C. H. J Appl Polym Sci 1999, 74, 1635.
9. Ghaemy, M.; Khandani, M. H. Eur Polym J 1998, 34, 477.
10. May, C. A. Epoxy Resins: Chemistry and Technology; Marcel Dekker: New York, 1988.
11. Faraga, F.; Burgo, S.; Nunez, E. R. J Appl Polym Sci 2001, 82, 3366.
12. Don, T. M.; Bell, J. P. J Appl Polym Sci 1998, 69, 2395.
13. Ghaemy, M.; Omrani, A.; Rostami, A. A. J Appl Polym Sci 2005, 97, 265.
14. Hummel, D. O.; Solti, A. Atlas of Polymers and Plastics; VCH: New York, 1988; Vols. 1–2.
15. Conley, R. T. Infrared Spectroscopy; Allyn and Bacon: Boston, 1972.
16. Sewell, G. J.; Billingham, N. C.; Kozielski, K. A.; George, G. A. Polymer 2000, 41, 2113.
17. Nunez, L.; Taboada, J.; Fraga, F.; Nunez, M. I. Appl Polym Sci 1997, 66, 1377.
18. Barton, J. M. Adv Polym Sci 1985, 72, 111.
19. Horie, K.; Hiura, H.; Sawada, M.; Mita, I.; Kambe, H. J Polym Sci Part A: Polym Chem 1970, 8, 1357.
20. Moroni, A.; Mijovic, J.; Pearce, E.; Foun, C. C. J Appl Polym Sci 1986, 32, 3761.
21. Khanna, U.; Lyer, R. J Appl Polym Sci 1993, 49, 319.
22. Golub, M. A.; Lerner, N. R. J Appl Polym Sci 1986, 32, 5215.
23. Barton, J. M. Polymer 1980, 21, 603.
24. Ryan, M. E.; Dutta, A. Polymer 1979, 20, 203.
25. Kenny, J. M. J Appl Polym Sci 1994, 51, 761.
26. Mijovic, J.; Kim, J.; Slaby, J. J Appl Polym Sci 1984, 29, 1449.
27. Eyring, H. J Chem Phys 1935, 3, 107.
28. Evans, G.; Polyani, M. Trans Faraday Soc 1935, 31, 875.